

New Model for Predicting Adsorption of Polar Molecules in Metal–Organic Frameworks with Unsaturated Metal Sites

Christopher Campbell,[†] José R. B. Gomes,[‡] Michael Fischer,^{§,||} and Miguel Jorge^{*,†,||}

[†]Department of Chemical and Process Engineering, University of Strathclyde, 75 Montrose Street, Glasgow G1 1XJ, Scotland, United Kingdom

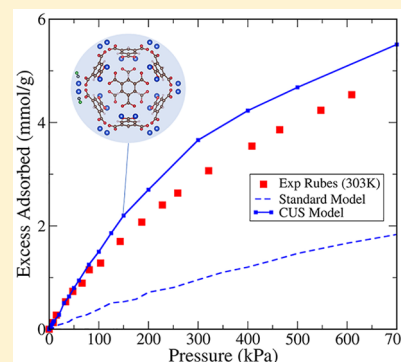
[‡]CICECO- Aveiro Institute of Materials, Department of Chemistry, University of Aveiro, Campus Universitário de Santiago, 3810-193 Aveiro, Portugal

[§]Crystallography Group, Department of Geosciences, University of Bremen, Klagfurter Straße, 28359 Bremen, Germany

^{||}MAPEX Center for Materials and Processes, University of Bremen, 28359 Bremen, Germany

S Supporting Information

ABSTRACT: Conventional molecular models fail to correctly describe interactions of adsorbates with coordinatively unsaturated sites (CUS) present in a large number of metal–organic frameworks (MOFs). Here, we confirm the failure of these models for a prototypical polar adsorbate, carbon monoxide, and show that simply adjusting their parameters leads to poor agreement with experimental isotherms when outside the fitting conditions. We propose a new approach that combines quantum mechanical density functional theory (DFT) with Monte Carlo simulations to rigorously account for specific interactions at the CUS. By explicitly including electrostatic interactions and employing accurate DFT functionals that describe dispersion interactions, our modeling approach becomes generally applicable to both polar and nonpolar molecules. We demonstrate that this CUS model leads to substantial improvement in carbon monoxide adsorption isotherm predictions, and correctly captures the coordination binding mechanism. This paper represents a major stepping stone in the development of a robust, transferable and generally applicable approach to describe the complex interactions between gas molecules and CUS, with great potential for use in large-scale screening studies.



Metal–organic frameworks (MOFs) are the focus of many recent studies due to their potential role in a variety of applications. They can have extremely high porosities and surface areas, as well as unique binding sites.¹ These attributes, combined with the ability to tailor MOFs through metal and ligand selection, promote them as ideal candidates for challenging gas separations. The focus of this research is on a subset of MOFs that contain coordinatively unsaturated sites (CUS), also known as open metal sites (OMS). These sites form when the metals are not fully coordinated to ligands but are also bound to guest molecules, e.g., solvent, in the as-synthesized form. Upon preadsorption activation, these molecules can be removed, leaving free CUS. These sites are then able to form strong coordination bonds with certain adsorbates that are able to donate electrons to the metal atoms. This selectivity feature of CUS has already been exploited to separate mixtures of physically similar gases, e.g. ethane/ethylene, which are hard to separate using other means.²

Due to the sheer number of potential combinations of linkers and metals, the number of available MOFs is extremely high. Screening this huge number of possible structures for a particular gas separation using experimental techniques is prohibitively costly and time-consuming. For this reason, high-throughput computational screening approaches that have recently emerged^{3,4} could play a pivotal role in assessing

performance of MOFs for gas separations prior to more detailed experimental studies. A caveat to the success of these strategies is the well-documented failure of conventional molecular models in accounting for the coordination interaction between CUS and certain gas molecules.^{5–9} This has led to large underestimations of simulated adsorption isotherms when compared to experiment for those adsorbates in which this interaction plays a key role, e.g. ethylene. In recent years, a few approaches that make use of quantum mechanical (QM) calculations in combination with classical grand-canonical Monte Carlo (GCMC) simulations were proposed to deal with this limitation.^{10–13} These approaches were recently reviewed,^{5,7} and the reader is referred to those articles for a more detailed discussion. Our particular strategy^{5–7,11} restricts the use of QM to describe the local interaction at the CUS, while relying on standard molecular models to describe interactions with the remainder of the framework. This enhances the transferability of the model in comparison with alternative approaches,^{12,14} and we believe this is essential for a CUS model to be viable for high-

Received: March 29, 2018

Accepted: June 9, 2018

Published: June 10, 2018

throughput screening simulations. Indeed, our previous work showed that the model is both transferable to chemically similar adsorbates (ethylene to propylene)⁶ and to different MOFs with the same CUS unit.⁵ No such transferability has yet been demonstrated for other CUS modeling approaches.

Our previous work focused solely on nonpolar adsorbates, ignoring electrostatic interactions for simplicity. Here, we generalize our approach to deal with polar adsorbates for which electrostatic interactions are important. We have chosen carbon monoxide as a test case due to its simplicity and importance in practical applications. Carbon monoxide is a gas present in a variety of industrial sectors. It is commonly formed as an unwanted byproduct in incomplete combustion reactions of various oil and gas mixtures.¹⁵ Therefore, its removal from these streams is an important step in reducing pollution. Carbon monoxide can, however, also be a valuable feedstock. It is often produced from either coal gasification or steam reforming, as a component of synthesis gas mixtures (mainly made up of H_2 :CO).¹⁶ This is because for many industrial uses, such as the industrial production of methanol, aliphatic alcohols and aldehydes, it is advantageous to have both gases present; also CO is an important reducing agent within metal refining.^{16,17} However, the correct ratio of H_2 :CO must first be obtained for many of these applications, requiring cost-effective gas separations, in which MOFs could play a role. Furthermore, for many applications, the use of pure carbon monoxide is required or industrially preferable, importantly, as a primary component in the production of acetic acids.¹⁶ The separation of pure carbon monoxide from a gas mixture, such as synthesis gas, becomes much more demanding when attempting to remove any nitrogen components. This is due to the similar boiling points of carbon monoxide ($\approx -192^\circ\text{C}$)¹⁸ and nitrogen ($\approx -196^\circ\text{C}$),¹⁸ making distillation separation costly and difficult.

The main challenge faced in simulating polar gases, like CO, with our DFT/GCMC coupled approach is that we will now need to account for the effect of electrostatics in the isolation of the local CUS interaction, as discussed in more detail later. We will also improve our approach by applying a DFT method that accurately accounts for dispersion interactions through the use of the vdW-DF2¹⁹ exchange-correlation functional. This is an important step in reducing the number of approximations required in our previous work,⁵ which was based on energies obtained with the PBE²⁰ exchange-correlation functional that were assumed to include no dispersion contributions. The step of extending the model to polar adsorbates is crucial to fully establishing the transferability and generality of our approach. To this end, we also performed calculations for ethylene to demonstrate that transferability is retained with the new procedure. This paper will show that our model can indeed provide good quantitative agreement with experiment and can potentially be used as an important tool for predicting MOF selectivity in gas mixtures that include both polar and nonpolar components.

As carbon monoxide has orbitals with electron-donating capabilities, it will interact strongly with CUS sites. For example, Bordiga et al.²¹ experimentally studied CO adsorption in HKUST-1 MOF, and found that electrostatics alone was unable to account for the interaction with the copper atoms, and that a π -metal interaction was taking place. We computed the adsorption energy profiles for CO adsorption at the unsaturated Cu site of HKUST-1²² using DFT. The binding energies and distances at the energy minima are shown

in Table 1 for each of the DFT calculations (the PBE functional was included to enable direct comparison with our

Table 1. DFT Energy Minima for Each Adsorbate Using Different DFT Exchange-Correlation Functionals (E_{xc})

E_{xc}	adsorbate	energy (kJ/mol)	BD ^a (Å)
PBE	carbon monoxide	−23.0	2.24
vdW-DF2	carbon monoxide	−28.8	2.32
PBE	ethylene	−23.3	2.61
vdW-DF2	ethylene	−36.4	2.65

^aBD is the closest binding distance to the Cu atom; for CO it is taken with respect to the carbon atom, while for ethylene it is relative to the midpoint of the C=C double bond.

previous approach^{5–7,11}). The adsorption energy found for carbon monoxide is nearly as strong as that of ethylene, confirming that the CUS plays a crucial role in carbon monoxide adsorption. Additionally, the binding energy of ≈ 29 kJ/mol for carbon monoxide in HKUST-1, found with vdW-DF2, is promising as it matches the experimental enthalpy of adsorption found by Rubeš et al. (29 kJ/mol).²³ Furthermore, an increase in the DFT adsorption energy for ethylene from PBE, −23.3 kJ/mol, to the vdW-DF2 case, −36.4 kJ/mol, should be noted, suggesting that dispersion is being accounted for in the latter case.

The binding orientations for the vdW-DF2 energy minima can be seen in Figure 1a,b. The orientations shown for carbon monoxide and ethylene at the minimum energy are the same for both exchange-correlation functionals. We have examined several other possible orientations for the CO molecule at the CUS (see the Supporting Information, Figure S1). The most favorable orientation, shown in Figure 1b, involves adsorption parallel to the Cu–Cu vector, with the carbon atom closest to the metal. This agrees closely with a relatively recent DFT study conducted by Supronowicz et al.²⁴

Together with previous studies,^{21,23} our DFT results show that accurately modeling CO adsorption in MOFs will require CUS interactions to be accounted for within GCMC simulations. In the literature there is surprisingly little in terms of adsorption simulations of carbon monoxide in MOFs, especially on CUS-containing MOFs.^{25–30} Fischer et al.³⁰ investigated the performance of existing CO models in GCMC simulations, and used the best performing model to predict adsorption in MOFs for CO/ H_2 separation. Karra et al.^{26,29} also used GCMC simulations to predict CO/ N_2 separations in HKUST-1 without explicitly accounting for any CUS interaction, and appeared to obtain good agreement with experiment. However, more recent work by Martín-Calvo et al.²⁷ illustrated that using the same model led to underestimation by simulation in the low pressure region, in which solid–fluid interactions dominate. Those authors²⁷ subsequently developed a new CO model that was fitted to experimental vapor–liquid equilibrium data.

In this work, several existing models will be tested for CO adsorption in MOFs to choose the most suitable model for further study. Martín-Calvo et al.²⁷ carried out a comprehensive comparison of CO models for their ability to predict vapor–liquid equilibrium, and we will use their study as a basis for our assessment. In particular, they examined four different models, UFF,³¹ Straub and Karplus³² (S&K), Piper et al.,³³ and their own model, which we will call the M-C model.²⁷ Of these, the UFF and M-C models showed the best agreement

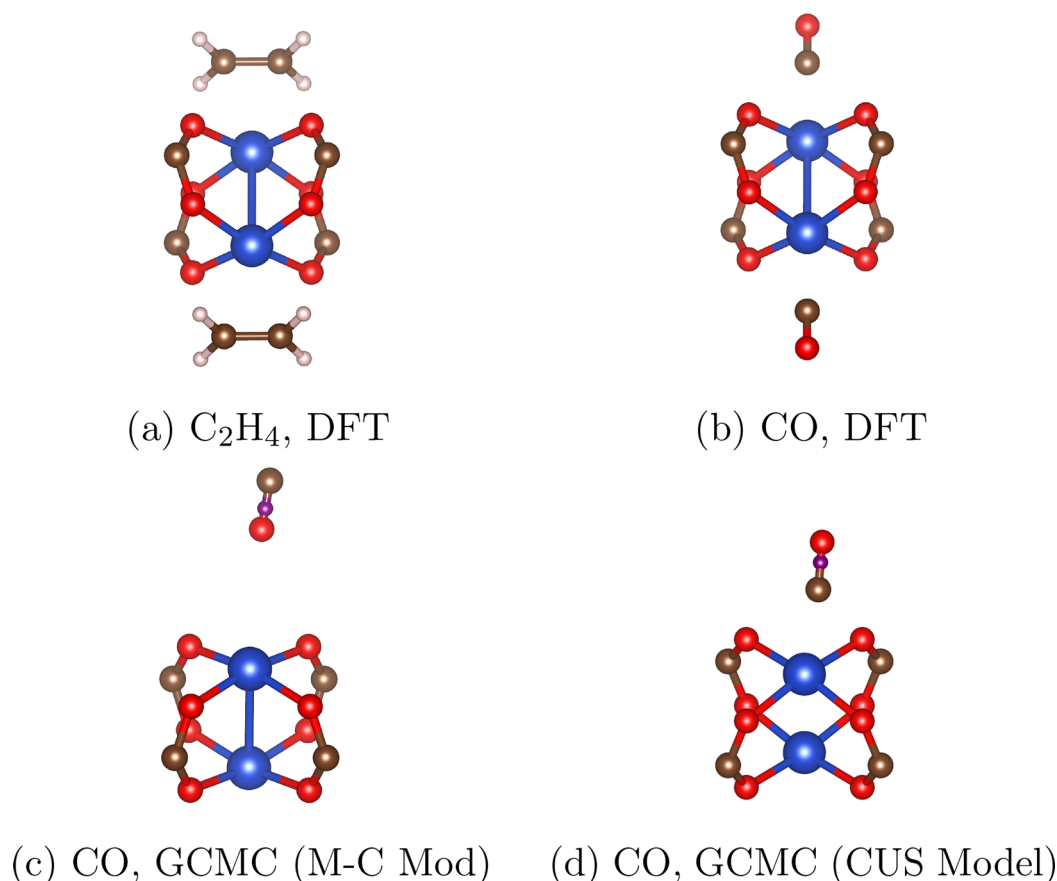


Figure 1. Diagram showing the binding orientations of the adsorbates with respect to the CUS using different modeling approaches: (a) ethylene from DFT; (b) CO from DFT; (c) CO from GCMC simulation using the modified M-C model (303 K and 700 kPa); (d) CO from GCMC simulations using our new CUS model (303 K and 100 kPa). Color code for atoms is blue - copper, red - oxygen, brown - carbon, white - hydrogen, and purple - dummy electrostatic site.

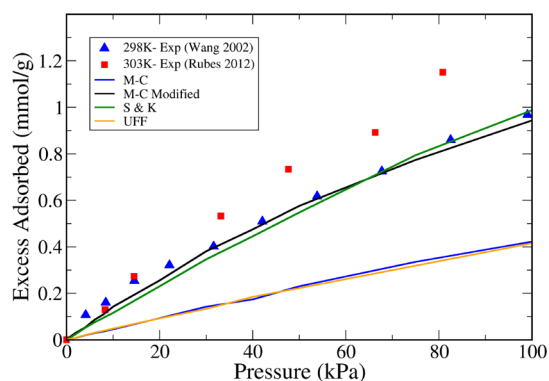
with liquid–vapor equilibrium data.²⁷ The S&K model uses the same geometry as M-C, but the different parameters lead to a much poorer performance in vapor–liquid equilibrium simulations. The Piper et al.³³ model was not investigated further here, as it uses a complex four-site point charge geometry, making it challenging for later combination with our CUS model, and also performed poorly in liquid–vapor equilibrium simulations. The Lennard-Jones (LJ) parameters and point charges for all CO models considered can be found in Table S1, and a visual representation of the site layouts is shown in Figure S2.

Martín-Calvo et al.²⁷ also proposed a modified model in which the LJ ϵ values for the CO–MOF interaction were increased by a factor of 1.2 relative to the standard mixing rules, and some of the mixed σ values were very slightly altered, in order to match CO adsorption in HKUST-1 at 298 K. The CO–MOF parameters for this modified M-C model are shown in Table S2 together with parameters obtained with the standard Lorentz–Berthelot combining rules to enable direct comparison. Here we will compare the performance of these models for predicting adsorption of CO in HKUST-1, but also in MOF-5,³⁴ or IRMOF-1, as an example of a widely studied MOF without CUS. In particular, we will assess the performance of the models against high pressure experimental adsorption data of CO in HKUST-1, which was not available at the time of the Martín-Calvo study.

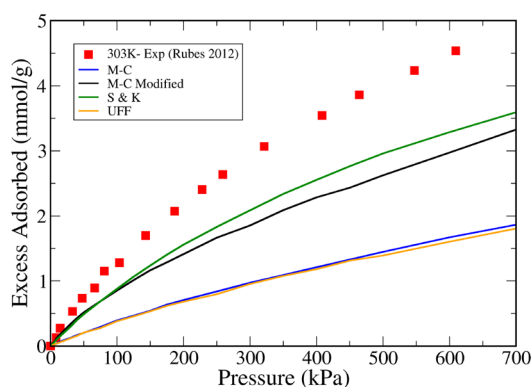
In agreement with Martín-Calvo et al.,²⁷ both the UFF and M-C models largely underestimate adsorption at all conditions

when compared with both sets of HKUST-1 experimental data (Figure 2a,b). As both models replicate vapor–liquid equilibrium data very well,²⁷ this is unlikely due to the gas–gas interactions and is caused instead by not accounting for specific interactions with the CUS of the MOF, which these force fields were not designed to describe. Unsurprisingly, the modified M-C model performs well in comparison with experimental adsorption at 298 K (Figure 2a), since the scaling parameters for CO–MOF interactions were designed to fit this particular data set. This scaling uniformly enhances dispersion interactions between CO and all the framework atoms (see Table S2), leading to higher adsorption. The S&K model also shows good agreement with experiment at 298 K, but this is now due to the much higher values of the CO point charges (see Table S1), leading to stronger electrostatic interactions with the framework (see Figure S3). The price of these enhanced electrostatics is a much poorer performance in vapor–liquid equilibrium simulations.²⁷ Therefore, error cancellation between gas–gas and gas–solid interactions is the most likely explanation for the rather fortuitous adsorption agreement at 298 K in the case of the S&K model.

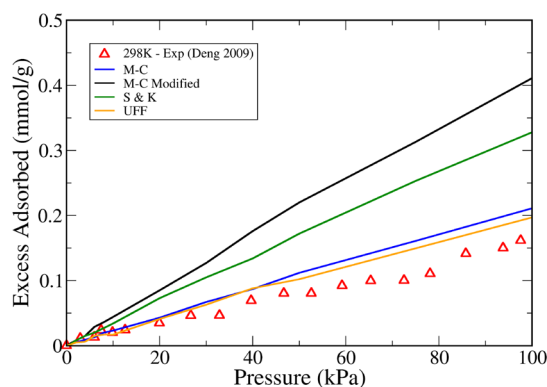
Although the modified M-C model closely agrees with the Wang experimental data set,³⁵ to which it was fitted, it is not able to match the isotherm of Rubeš et al.²³ at 303 K (Figure 2b). In fact, Figure 2a clearly shows that the Wang et al. isotherm has a lower adsorbed amount than that of the more recent work of Rubeš et al., despite the latter corresponding to a slightly higher temperature (303 K). This is true even after



(a) Low Pressure, HKUST-1



(b) High Pressure, HKUST-1



(c) Low Pressure, IRMOF-1

Figure 2. Simulated (lines) and experimental (symbols) carbon monoxide adsorption isotherms in HKUST-1 [(a) 298 K; (b) 303 K] and IRMOF-1 [(c) 298 K]. In panel a, the experimental data are from Wang et al.³⁵ In panel b, the experimental data are from Rubeš et al.²³ In panel c, the experimental data are from Deng et al.³⁶

scaling for pore volume differences in the two experimental samples, as described in the [Computational Methods](#) section. This suggests that the much earlier Wang et al. data were likely obtained on a lower quality sample of HKUST-1, and highlights the pitfalls of fitting force field parameters to match a restricted set of experimental data without subsequent validation.⁹

Figure 2b shows that none of the available models is able to capture the correct high-pressure saturation behavior. This is because no model is able to describe the binding mechanism at the CUS correctly. Indeed, none of the investigated models

showed a strong preference for binding at the CUS, which DFT calculations (Table 1) identified as a highly attractive site. Furthermore, even when interactions between CO and the CUS were observed, the opposite orientation was obtained when compared with the DFT-optimized geometry. Figure 1c shows a simulation snapshot obtained at 303 K and 7 bar using the modified M-C model, focusing on the area around the Cu paddlewheel unit. Compared to the DFT geometry from Figure 1b, the binding distance is much larger and, more importantly, it is the oxygen atom that is closest to the CUS, instead of the carbon atom as observed in DFT. As shown in Tables S1 and S2, almost all models have oxygen with a higher ϵ value than that of carbon (the exception being UFF) and also a more negative point charge, making the oxygen's LJ potential and electrostatics both more attracted to the Cu atoms, which have been assigned a positive point charge. It should also be noted that the configuration shown in Figure 1c is actually quite rare in all simulations with the standard models. This analysis confirms that the standard models are not capturing the correct adsorption mechanism of CO at the CUS, which hinders their ability to accurately predict adsorption isotherms over a wide range of conditions.

As illustrated in Figure 2c, in the case of IRMOF-1, in which no CUS are present, a very different picture can be seen. The UFF and M-C models now provide relatively good agreement with experiment across the full isotherm. This, in conjunction with the HKUST-1 results, further reinforces the idea that these models are capturing the gas–gas interaction correctly, as well as the standard van der Waals and electrostatic interactions with the solid. They fail when CUS are present in the MOFs, which is to be expected, and this makes both of them good candidates for combining with the CUS model proposed here. The failure of the modified M-C model shows that, although strengthening the LJ parameters improves agreement in HKUST-1 at low pressure, the parameters cannot be transferred to IRMOF-1. This raises doubts about the possibility of generally transferring this model to other MOFs (both with and without CUS) without further parameter fitting.

Based on the above results, we are now in a position to select the most appropriate CO model to be combined with the QM-based CUS interaction. When looking at the performance of the UFF and M-C models, both replicate vapor–liquid equilibrium data well²⁷ and also both appear to capture the van der Waals and electrostatic interaction with IRMOF-1 correctly. The decision was made to use the M-C model for the CUS method due to it being able to better replicate the experimental dipole moment of the carbon monoxide molecule, with the M-C model exactly matching experiment at 0.112 D, while UFF is significantly higher at 0.58 D.²⁷

It was clearly shown that none of the existing CO models can fully describe the adsorption mechanism on HKUST-1, and that enhancing electrostatics or the LJ parameters fails to adequately correct for this. Furthermore, these techniques also lose backward compatibility for MOFs without CUS. Therefore, we will investigate if isotherm agreement can be improved by explicitly accounting for the CUS interaction through combining QM and GCMC. We will compare simulations only to the Rubeš et al. data set,²³ as it appears to be more reliable as discussed previously, and covers a wider pressure range.

The CO CUS model is built by isolating the CUS local interaction from the DFT adsorption energy profile, with this CUS local interaction profile then fitted to a modified Morse

potential for use in GCMC simulations. The CUS binding energies are isolated by removing the standard force field energies used within the GCMC simulations, i.e., the LJ potential and electrostatic potential (assumed to be negligible for ethylene). In our previous work's approach (PBE-based), the DFT calculations were assumed to contain no dispersion and therefore only the repulsive contribution of the LJ potential needed to be removed from the DFT profile. In the new procedure (vdW-DF2-based) the DFT profile contains dispersion interactions, and therefore the full LJ potential can be subtracted from the DFT profile, rather than requiring the repulsive contribution to be decoupled from the LJ potential. Further details of the CUS model can be found in the [Computational Methods](#).

When our previous CUS model is used, based on DFT calculations with the PBE functional, we observe a significant improvement relative to the standard models, but simulations now significantly overestimate adsorption ([Figure 3](#)). This was

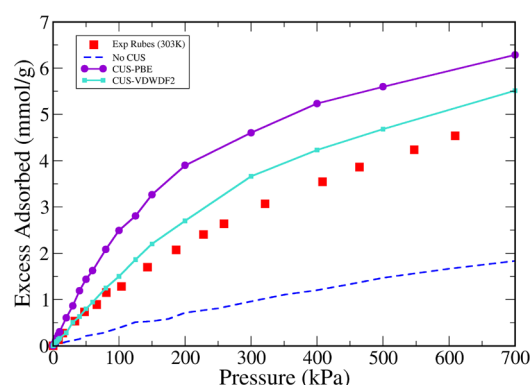


Figure 3. CUS model simulated (lines), non-CUS model simulated (dashed line), and experimental²³ (points) carbon monoxide adsorption isotherms in HKUST-1.

initially surprising, as this procedure had been successfully used to predict ethylene adsorption in the same MOF,⁵ and suggests that the assumption that PBE energies contain no dispersion contribution is not entirely valid in the case of CO. As can be seen in [Figure 3](#), the CUS model derived from the vdW-DF2 functional, based on an accurate treatment of dispersion interactions, provides much better agreement with experiment throughout the entire pressure region.

[Figure 4](#) shows selected simulation snapshots of CO adsorption in HKUST-1. At very low pressures, as expected from our DFT calculations, the CUS is the preferred binding site for CO molecules ([Figure 4a](#)). This is in contrast to predictions using standard models,²⁷ where CO was seen to adsorb first in the small cages. As the pressure increases, the small cages begin to be populated as they also present strong adsorption energies ([Figure 4b](#)). At higher pressure ([Figure 4c,d](#)), CO molecules occupy a variety of sites, with a relative preference in the order CUS > small cages > large cages.

To further validate our improved protocol for including the CUS interaction, it was also applied to the previously studied case of ethylene adsorption in HKUST-1. The ethylene parameters obtained with the new protocol will also be transferred to a different copper paddlewheel MOF (PCN-16) to confirm that the CUS model's transferability demonstrated by Campbell et al.⁵ is maintained. As shown in [Figure 5a](#), the new procedure, utilizing vdW-DF2, leads to practically

identical results as obtained with PBE for this system. This arises directly from the similar minimum energy binding distances obtained with the two DFT approaches (binding distances are PBE 2.61 Å and vdW-DF2 2.65 Å) and similar CUS specific interaction (PBE −38 kJ/mol, after adding dispersion, and vdW-DF2 −39 kJ/mol). The good agreement with experiment demonstrates the generality of our new approach over both polar and nonpolar adsorbates. Furthermore, using the exact same parameters for the CUS interaction obtained in HKUST-1 leads to very good predictions of adsorption in PCN-16 ([Figure 5b](#)), again with negligible differences from previous work. This highlights that the new procedure retains the same transferability demonstrated for copper paddlewheel MOFs. In [Figures S5 and S6](#), it is also shown that the CUS model is relatively insensitive to the choice of framework point charges, and the adsorption isotherm is only slightly affected.

In summary, in this paper we have shown that existing carbon monoxide models are unsuitable for capturing the orbital behavior of CUS-containing MOFs, and consequently agree poorly with experimental adsorption isotherms for HKUST-1. Furthermore, attempts to improve agreement through adjustment of LJ parameters fail to find agreement across the full isotherm, and also lose backward compatibility with non-CUS containing MOFs. This work builds upon our group's CUS model, which has been shown to be transferable across adsorbates (ethylene to propylene)⁶ and adsorbents (copper paddlewheel MOFs).⁵ It has now been successfully extended to polar adsorbates (carbon monoxide) and, through removal of dispersion-related assumptions, agrees closely with experiment across the full isotherm. Importantly, it also captures the correct binding mechanism at the CUS, which is required for accurate simulation of competitive binary adsorption. The updated procedure was also back-validated successfully against previous work,⁵ to ensure that transferability was indeed retained. Overall, this work highlights the robust nature of this CUS approach and its flexibility across different adsorbent and adsorbate types, making it an ideal candidate for use in large-scale computational screening of MOFs for gas separations.

COMPUTATIONAL METHODS

Dispersion and repulsion interactions were described through the standard Lennard-Jones 12–6 potential. Parameters from the DREIDING force field³⁸ were used to describe all the MOF framework atoms apart from copper. Parameters for copper atoms are not present in DREIDING and therefore the Universal force field (UFF) was used.³¹ This combination of parameters has been successfully used to model adsorption in MOFs without CUS.³⁹ The point charges used to describe the framework's electrostatic interaction were those of Castillo et al.,⁴⁰ which have been used previously for carbon monoxide adsorption simulations in MOFs.²⁷ For ethylene, a united atom approach was used for each CH₂ group, with parameters taken from the TraPPE force field.^{41,42} This force field was selected as it is fitted against vapor–liquid equilibrium data, helping to ensure that the gas–gas interactions are correctly captured and thus enabling the focus of this research to be solely on the gas–solid interactions. Furthermore, the TraPPE force field has been used previously to describe adsorption of alkenes and alkanes in MOFs.^{5,6,13,43,44} With the exception of the modified M-C model,²⁷ all cross-species LJ interactions were estimated using the standard Lorentz–Berthelot combining rules.

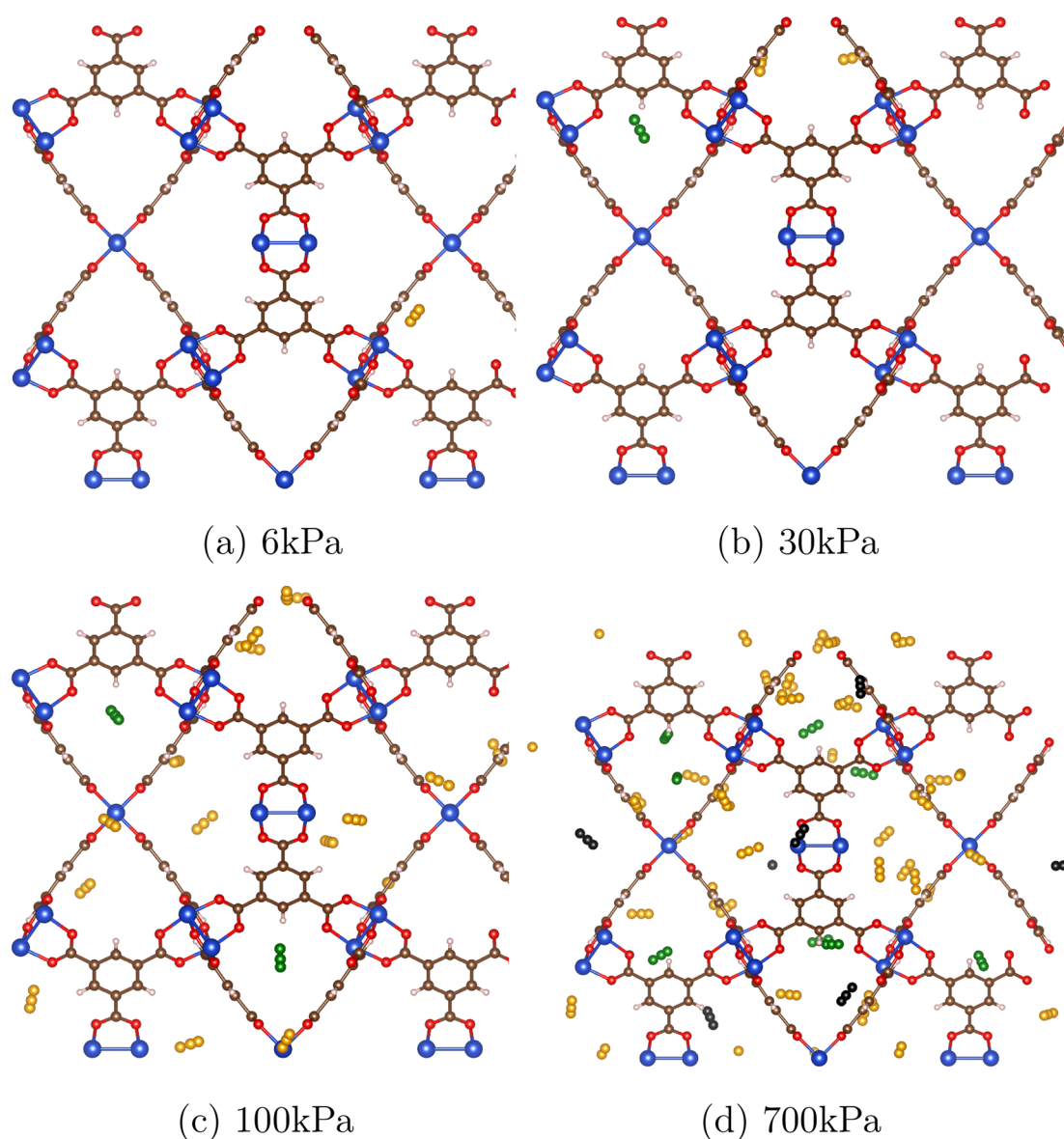


Figure 4. Diagram showing the filling of the HKUST-1 framework at different pressure points throughout the GCMC CUS model simulations (303 K). Color code for atoms is blue - copper, red - oxygen, brown - carbon, white - hydrogen, yellow - CO binding to CUS, black - CO adsorption on large cage, and green - CO adsorption on small cage. We note that the simulation box is periodic in all three directions of space.

Adsorption isotherms were obtained through GCMC simulations using the open source code Music.⁴⁵ All framework and adsorbate atoms were kept rigid, and an interaction cutoff distance of 13 Å was applied for the LJ interactions. Ewald summations were applied in all solid–fluid electrostatic interactions, while fluid–fluid electrostatic interactions were described using the Wolf summation method.⁴⁶ We made use of pretabulated grids (PMAPs) to speed up the calculation of solid–fluid LJ and electrostatic interactions, with a grid spacing of 0.15 Å. For all GCMC simulations that did not include CUS interactions, cavity bias⁴⁷ based on the LJ PMAP was used for insertion and deletion trials. In the case of simulations explicitly including CUS interactions, insertion and deletion were done randomly. In addition to insertion and deletion trials, molecules were allowed to rotate and translate, using optimized maximum displacements. 600 000 000 steps were used for all non-CUS model GCMC simulations and 100 000 000 were used for all CUS model GCMC simulations.

[Note: in the case of the S&K model for CO (see Table S1) due to a memory allocation error within the Music version, bias insertion could not be used; to compensate for this, the number of steps was increased to 1 000 000 000.] The first 50% of steps were ignored to ensure equilibration, and the remaining steps were split into 20 equal blocks for error analysis. Pressure values were converted to fugacities for input into the simulation code using the Peng–Robinson equation of state.⁴⁸ The final absolute adsorbed amounts from the simulations were converted to excess, for comparison with experiment, using the Myers and Monson method.⁴⁹ Furthermore, except where noted, experimental adsorption isotherms were scaled by the ratio of the theoretical over experimental nitrogen pore volumes, so that they can be directly compared to GCMC simulations on a perfect crystal. A more detailed discussion of the pore volume scaling procedure can be found in the Supporting Information, and previous work.⁶

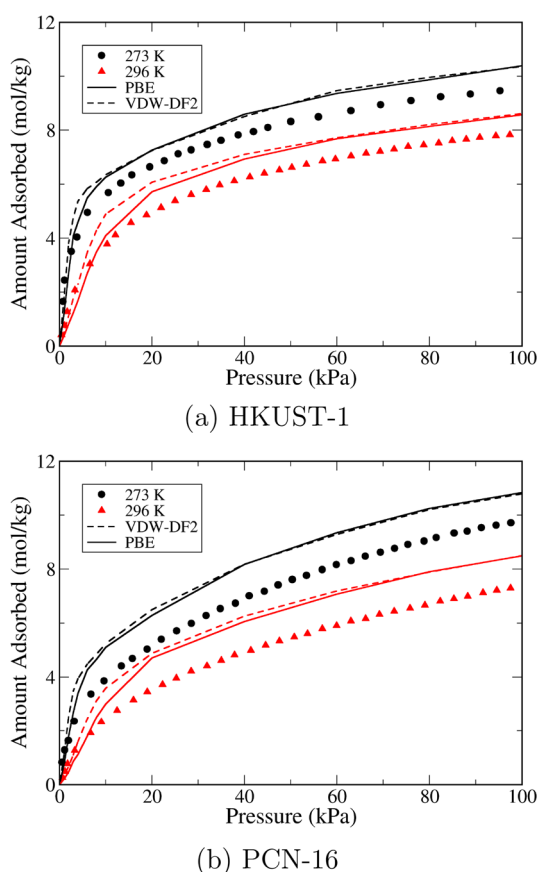


Figure 5. Simulated (lines) and experimental (symbols),³⁷ ethylene adsorption isotherms in (a) HKUST-1 and (b) PCN-16.

The CUS approach has been described in detail in previous work,^{5,6,11} therefore here we will focus on the changes to the procedure that generalize it to handle polar molecules. The procedure comprises 5 key stages:

1. Quantum-mechanical calculations to obtain the adsorption energy profile between the adsorbate and the CUS.
2. Isolation of the CUS contribution from the DFT profile.
3. Fitting the resulting profile to a modified Morse potential.
4. Including the new CUS interaction site in GCMC simulations.
5. Validating GCMC adsorption isotherms against experiment.

For the DFT calculations, in our previous work⁵ we used the PBE exchange-correlation functional,²⁰ which was assumed to account for no dispersive interactions. Here, we relax this assumption by applying a DFT functional that accurately accounts for dispersion. There are two commonly used approaches to account for dispersion interactions within DFT calculations, using an explicit correction term or implicitly accounting for it within the exchange-correlation functional.⁵⁰ The former approach can be successfully applied with functionals assumed to have little to no dispersive interaction, and can even be combined with dispersion-including functionals if they are thought not to fully capture the long and short-range of the dispersive interaction.⁵¹ However, the success of this approach is very dependent on the system being studied and can also involve partially scaling the correction⁵¹ when applied to exchange-correlation func-

tionals already partially capturing dispersion, which adds an empirical nature to the procedure. As such, the decision was made to focus on exchange-correlation functionals that implicitly account for dispersion. The vdW-DF2¹⁹ was selected as it has been successfully employed in force field development for MOFs, and provided better agreement with MOF experimental isotherms than an approach utilizing PBE-D2⁵²-corrected DFT calculations.¹³ We also carried out calculations with PBE for comparison with our previous approach.

DFT calculations with the PBE²⁰ exchange-correlation functional were carried out with CP2K software⁵³ using a similar protocol as in our previous work.⁵ The basis sets used for all but the Cu atoms were triple- ζ plus polarization (TZVP) with PBE-optimized Goedecker pseudopotentials.^{54–56} These basis sets were unavailable for copper, and therefore the double- ζ plus polarization (DZVP) sets were used. The energy cutoff selected for PBE was 600 Ry, and spin polarization was included. Furthermore, a single point counterpoise correction⁵⁷ was used to account for basis set superposition error (BSSE). The importance of BSSE for carbon monoxide calculations was much higher than that of the previous ethylene DFT calculations⁵—for PBE optimization calculations at the minimum, the BSSE corrections for ethylene and carbon monoxide were ≈ 2 kJ/mol and ≈ 14 kJ/mol, respectively.

Because vdW-DF2¹⁹ was not available in CP2K, Quantum Espresso⁵⁸ DFT calculations using the nonlocal correlation vdW-DF2 functional were performed with the periodic PWSCF v.5.3.0 code, using the same DFT optimization procedure as outlined in Campbell et al.⁵ Plane-wave basis sets were used to describe the valence electrons together with norm-conserving pseudopotentials within the Troullier-Martins approach for the core electrons.⁵⁹ It should be noted that as plane-wave basis sets are being used there will be no BSSE error present. The Kohn–Sham orbitals were expanded with 50 Ry cutoff for the kinetic energy and 200 Ry cutoff for the charge density. The first Brillouin zone integrations were performed with the Marzari–Vanderbilt smearing method at the gamma point. The convergence criteria were as follows: convergence threshold for self-consistency was 1×10^{-6} Ry (using a local-density-dependent Thomas–Fermi screening mixing mode with a factor of 0.7 for self-consistency) and convergence on forces was 1×10^{-3} Ry/au.

Once each adsorption energy profile for the adsorbate with respect to the CUS has been determined, the CUS contribution must be isolated. The exact method for this isolation depends on the adsorbate and exchange correlation functional being used. In the case of ethylene, it is assumed that electrostatics do not play a significant role in adsorption in MOF frameworks.^{5,6} This assumption is not valid for carbon monoxide, as discussed, and therefore the electrostatic energies must also be subtracted from the DFT profile. Furthermore, the PBE functional is assumed to not account for dispersion interactions and therefore only the repulsive contribution from the LJ potential must be subtracted from the DFT profile. This is achieved by applying the Weeks–Chandler–Andersen (WCA) approximation^{60,61} on the LJ potential. With vdW-DF2, the dispersion term should also be removed from the DFT profile. Therefore, the dispersion and repulsion contributions can simply be removed together through the standard LJ potential, eliminating the need for the WCA approximation. The variations in the isolation forms for each of the systems can be seen in eqs 1–4.

Table 2. CUS Parameters Obtained from DFT Fitting to eqs 1 to 5

E_{xc}	adsorbate	R_0 (Å)	D_0 (kJ/mol)	α	A	B
PBE	carbon monoxide	2.7712	10.3400	9.0376	3.3025	10.1583
PBE	ethylene	3.1030	10.6324	8.0945	3.8250	9.2812
vdW-DF2	carbon monoxide	2.7500	9.8290	8.2500	3.2430	10.1068
vdW-DF2	ethylene	3.0374	11.2000	8.4890	3.8246	9.2875

PBE: Ethylene

$$U_{Cu-\pi}(r) = U_{DFT}(r) - \frac{U_{Rep}(r)}{WCA} - \frac{U_{Disp}(r) - U_{Electro}(r)}{Zero} \quad (1)$$

PBE: Carbon Monoxide

$$U_{Cu-\pi}(r) = U_{DFT}(r) - \frac{U_{Rep}(r)}{WCA} - \frac{U_{Disp}(r)}{Zero} - U_{Electro}(r) \quad (2)$$

vdW-DF2: Ethylene

$$U_{Cu-\pi}(r) = U_{DFT}(r) - \frac{U_{Rep}(r)}{LJ\ Potential} - \frac{U_{Disp}(r)}{Zero} - \frac{U_{Electro}(r)}{Zero} \quad (3)$$

vdW-DF2: Carbon Monoxide

$$U_{Cu-\pi}(r) = U_{DFT}(r) - \frac{U_{Rep}(r)}{LJ\ Potential} - U_{Disp}(r) - U_{Electro}(r) \quad (4)$$

For the isolation of the Cu- π interaction, all the other interaction terms must be known. This was achieved using an in-house software to calculate the LJ and electrostatic potential energy profiles along the Cu-Cu vector in a fully periodic structure, based on the classical models that will be used later in GCMC simulations (M-C model in the case of carbon monoxide and TraPPE in the case of ethylene).

The now isolated Cu- π energy profile represents the specific attraction between each adsorbate and the CUS site of the MOF. However, the interaction site used within GCMC to account for the CUS interactions must be decided upon. In the case of ethylene, a new interaction site was placed on the center of the ethylene double bond.⁵ For carbon monoxide, the carbon atom is the nearest binding site to the copper (see Figure 1b) and therefore will be the CUS interaction site used in GCMC simulations. The CUS interaction profile is then fitted to a modified Morse potential,⁵ shown in eq 5.

$$U_{function}(r) = D_0 \cdot \left[\exp\left(\alpha \left(1 - \frac{r}{R_0}\right)\right) - 2 \cdot \exp\left(\frac{\alpha}{2} \left(1 - \frac{r}{R_0}\right)\right) \right] - \left(\frac{A}{r}\right)^B \quad (5)$$

where

R_0 = Distance of the minimum in the Morse potential (Å)

D_0 = Depth of this minimum (kJ/mol)

α = Flexibility of the fitting curve

A/B = Empirical power-law terms

The CUS parameters derived from the fitting procedure for each of the studied exchange correlation functionals are presented in Table 2. In the case of carbon monoxide the fluid-fluid force field selected was the M-C model, with framework point charges from Castillo et al.⁴⁰ The same cutoff

scheme as in previous work⁵ was used for the CUS model and can be found in the Supporting Information (eq S2 and Table S6).

■ ASSOCIATED CONTENT**Supporting Information**

The following files are available free of charge on the University of Strathclyde's data repository: Input files for all GCMC simulations and DFT calculations (<http://dx.doi.org/10.15129/9aceafff-a12f-421d-8317-0fa073ed35b4>). The Supporting Information is available free of charge on the ACS Publications website at DOI: 10.1021/acs.jpcllett.8b00967.

CO orientations - DFT calculations; CO GCMC model details; CO electrostatic interaction profiles; effect of framework point charges; experimental pore volume scaling details; CUS cut-off scheme (PDF)

■ AUTHOR INFORMATION**Corresponding Author**

*E-mail: miguel.jorge@strath.ac.uk.

ORCID

José R. B. Gomes: 0000-0001-5993-1385

Miguel Jorge: 0000-0003-3009-4725

Notes

The authors declare no competing financial interest.

■ ACKNOWLEDGMENTS

The authors thank A. Fletcher and F. Pelizza for helpful discussions. C.C. thanks EPSRC for a doctoral training grant (Award Reference EP/M506643/1 and EP/L505080/1). M.F. is funded by the Central Research Development Fund (CRDF) of the University of Bremen (Funding Line 04-Independent Projects for Post-Docs). J.R.B.G. is thankful to FCT/MEC and FEDER for Projects CICECO-Aveiro Institute of Materials, POCI-01-0145-FEDER-007679 (FCT ref. UID/CTM/50011/2013), and Investigador FCT.

■ REFERENCES

- (1) Zhou, H.-C.; Long, J. R.; Yaghi, O. M. Introduction to Metal-Organic Frameworks. *Chem. Rev.* **2012**, *112*, 673–674.
- (2) Bloch, E. D.; Queen, W. L.; Krishna, R.; Zadrozny, J. M.; Brown, C. M.; Long, J. R. Hydrocarbon Separations in a Metal-Organic Framework with Open Iron(II) Coordination Sites. *Science* **2012**, *335*, 1606–1610.
- (3) Wilmer, C. E.; Leaf, M.; Lee, C. Y.; Farha, O. K.; Hauser, B. G.; Hupp, J. T.; Snurr, R. Q. Large-scale Screening of Hypothetical Metal-Organic Frameworks. *Nat. Chem.* **2012**, *4*, 83–89.
- (4) Watanabe, T.; Sholl, D. S. Accelerating Applications of Metal-Organic Frameworks for Gas Adsorption and Separation by Computational Screening of Materials. *Langmuir* **2012**, *28*, 14114–14128.
- (5) Campbell, C.; Ferreira-Rangel, C. A.; Fischer, M.; Gomes, J. R. B.; Jorge, M. A Transferable Model for Adsorption in MOFs with Unsaturated Metal Sites. *J. Phys. Chem. C* **2017**, *121*, 441–458.

- (6) Jorge, M.; Fischer, M.; Gomes, J. R. B.; Siquet, C.; Santos, J. C.; Rodrigues, A. E. Accurate Model for Predicting Adsorption of Olefins and Paraffins on MOFs with Open Metal Sites. *Ind. Eng. Chem. Res.* **2014**, *53*, 15475–15487.
- (7) Fischer, M.; Gomes, J. R.; Jorge, M. Computational Approaches to Study Adsorption in MOFs with Unsaturated Metal Sites. *Mol. Simul.* **2014**, *40*, 537–556.
- (8) Liu, J.; Culp, J. T.; Natesakhawat, S.; Bockrath, B. C.; Zande, B.; Sankar, S. G.; Garberoglio, G.; Johnson, J. K. Experimental and Theoretical Studies of Gas Adsorption in $\text{Cu}_3(\text{BTC})_2$: An Effective Activation Procedure. *J. Phys. Chem. C* **2007**, *111*, 9305–9313.
- (9) Keskin, S.; Liu, J.; Rankin, R. B.; Johnson, J. K.; Sholl, D. S. Progress, Opportunities, and Challenges for Applying Atomically Detailed Modeling to Molecular Adsorption and Transport in Metal-Organic Framework Materials. *Ind. Eng. Chem. Res.* **2009**, *48*, 2355–2371.
- (10) Chen, L.; Grajciar, L.; Nachtigall, P.; Düren, T. Accurate Prediction of Methane Adsorption in a Metal-Organic Framework with Unsaturated Metal Sites by Direct Implementation of an ab Initio Derived Potential Energy Surface in GCMC Simulation. *J. Phys. Chem. C* **2011**, *115*, 23074–23080.
- (11) Fischer, M.; Gomes, J. R. B.; Fröba, M.; Jorge, M. Modeling Adsorption in Metal-Organic Frameworks with Open Metal Sites: Propane/Propylene Separations. *Langmuir* **2012**, *28*, 8537–8549.
- (12) Dzubak, A. L.; Lin, L.-C.; Kim, J.; Swisher, J. A.; Poloni, R.; Maximoff, S. N.; Smit, B.; Gagliardi, L. Ab Initio Carbon Capture in Open-Site Metal-Organic Frameworks. *Nat. Chem.* **2012**, *4*, 810–816.
- (13) Kulkarni, A. R.; Sholl, D. S. Screening of Copper Open Metal Site MOFs for Olefin/Paraffin Separations Using DFT-Derived Force Fields. *J. Phys. Chem. C* **2016**, *120*, 23044–23054.
- (14) Koh, H. S.; Rana, M. K.; Wong-Foy, A. G.; Siegel, D. J. Predicting Methane Storage in Open-Metal-Site Metal-Organic Frameworks. *J. Phys. Chem. C* **2015**, *119*, 13451–13458.
- (15) Speight, J. *Handbook of Industrial Hydrocarbon Processes*; Elsevier Science: New York, 2010.
- (16) Bierhals, J. *Ullmann's Encyclopedia of Industrial Chemistry*; Wiley-VCH Verlag GmbH and Co. KGaA: Weinheim Germany, 2000.
- (17) Peer, M.; Mehdi Kamali, S.; Mahdeyfar, M.; Mohammadi, T. Separation of Hydrogen from Carbon Monoxide Using a Hollow Fiber Polyimide Membrane: Experimental and Simulation. *Chem. Eng. Technol.* **2007**, *30*, 1418–1425.
- (18) Venanzi, T. J. Some Unusual Properties of Carbon Monoxide: A Comparison With N_2 . *J. Chem. Educ.* **1981**, *58*, 423.
- (19) Lee, K.; Murray, E. D.; Kong, L.; Lundqvist, B. I.; Langreth, D. C. Higher-Accuracy van der Waals Density Functional. *Phys. Rev. B: Condens. Matter Mater. Phys.* **2010**, *82*, 081101.
- (20) Perdew, J. P.; Burke, K.; Ernzerhof, M. Generalized Gradient Approximation Made Simple. *Phys. Rev. Lett.* **1996**, *77*, 3865–3868.
- (21) Bordiga, S.; Regli, L.; Bonino, F.; Groppo, E.; Lamberti, C.; Xiao, B.; Wheatley, P. S.; Morris, R. E.; Zecchina, A. Adsorption Properties of HKUST-1 Toward Hydrogen and Other Small Molecules Monitored By IR. *Phys. Chem. Chem. Phys.* **2007**, *9*, 2676–2685.
- (22) Chui, S. S. Y.; Lo, S. M.; Charmant, J. P. H.; Orpen, A. G.; Williams, I. D. A Chemically Functionalizable Nanoporous Material $[\text{Cu}_3(\text{TMA})_2(\text{H}_2\text{O})_3]_n$. *Science* **1999**, *283*, 1148–1150.
- (23) Rubes, M.; Grajciar, L.; Bludský, O.; Wiersum, A. D.; Llewellyn, P. L.; Nachtigall, P. Combined Theoretical and Experimental Investigation of CO Adsorption on Coordinatively Unsaturated Sites in CuBTC MOF. *ChemPhysChem* **2012**, *13*, 488–495.
- (24) Supronowicz, B.; Mavrandonakis, A.; Heine, T. Interaction of Small Gases with the Unsaturated Metal Centers of the HKUST-1 Metal Organic Framework. *J. Phys. Chem. C* **2013**, *117*, 14570–14578.
- (25) Sirjoosingh, A.; Alavi, S.; Woo, T. K. Grand-Canonical Monte Carlo and Molecular-Dynamics Simulations of Carbon-Dioxide and Carbon-Monoxide Adsorption in Zeolitic Imidazolate Framework Materials. *J. Phys. Chem. C* **2010**, *114*, 2171–2178.
- (26) Karra, J. R.; Walton, K. S. Effect of Open Metal Sites on Adsorption of Polar and Nonpolar Molecules in Metal-Organic Framework Cu-BTC. *Langmuir* **2008**, *24*, 8620–8626.
- (27) Martín-Calvo, A.; Lahoz-Martín, F. D.; Calero, S. Understanding Carbon Monoxide Capture Using Metal-Organic Frameworks. *J. Phys. Chem. C* **2012**, *116*, 6655–6663.
- (28) Valenzano, L.; Civalieri, B.; Chavan, S.; Palomino, G. T.; Areán, C. O.; Bordiga, S. Computational and Experimental Studies on the Adsorption of CO, N_2 , and CO_2 on Mg-MOF-74. *J. Phys. Chem. C* **2010**, *114*, 11185–11191.
- (29) Karra, J. R.; Walton, K. S. Molecular Simulations and Experimental Studies of CO_2 , CO, and N_2 Adsorption in Metal-Organic Frameworks. *J. Phys. Chem. C* **2010**, *114*, 15735–15740.
- (30) Fischer, M.; Hoffmann, F.; Fröba, M. Metal-Organic Frameworks and Related Materials for Hydrogen Purification: Interplay of Pore Size and Pore Wall Polarity. *RSC Adv.* **2012**, *2*, 4382–4396.
- (31) Rappe, A. K.; Casewit, C. J.; Colwell, K. S.; Goddard, W. A.; Skiff, W. M. UFF, A Full Periodic Table Force Field for Molecular Mechanics and Molecular Dynamics Simulations. *J. Am. Chem. Soc.* **1992**, *114*, 10024–10035.
- (32) Straub, J. E.; Karplus, M. Molecular Dynamics Study of The Photodissociation of Carbon Monoxide From Myoglobin: Ligand Dynamics In The First 10 ps. *Chem. Phys.* **1991**, *158*, 221–248.
- (33) Piper, J.; Morrison, J.; Peters, C. The Adsorption of Carbon Monoxide On Graphite. *Mol. Phys.* **1984**, *53*, 1463–1480.
- (34) Li, H.; Eddaoudi, M.; O'Keeffe, M.; Yaghi, O. M. Design And Synthesis of An Exceptionally Stable And Highly Porous Metal-Organic Framework. *Nature* **1999**, *402*, 276–279.
- (35) Min Wang, Q.; Shen, D.; Bülow, M.; Ling Lau, M.; Deng, S.; Fitch, F.; Lemcoff, N.; Semanscin, J. Metallo-organic Molecular Sieve For Gas Separation And Purification. *Microporous Mesoporous Mater.* **2002**, *55*, 217–230.
- (36) Saha, D.; Deng, S. Adsorption Equilibria and Kinetics of Carbon Monoxide on Zeolite 5A, 13X, MOF-5, and MOF-177. *J. Chem. Eng. Data* **2009**, *54*, 2245–2250.
- (37) He, Y.; Krishna, R.; Chen, B. Metal-organic Frameworks with Potential for Energy-efficient Adsorptive Separation of Light Hydrocarbons. *Energy Environ. Sci.* **2012**, *5*, 9107–9120.
- (38) Mayo, S. L.; Olafson, B. D.; Goddard, W. A. DREIDING: A Generic Force Field for Molecular Simulations. *J. Phys. Chem.* **1990**, *94*, 8897–8909.
- (39) Fang, H.; Demir, H.; Kamakoti, P.; Sholl, D. S. Recent Developments In First-Principles Force Fields For Molecules In Nanoporous Materials. *J. Mater. Chem. A* **2014**, *2*, 274–291.
- (40) Castillo, J. M.; Vlucht, T. J. H.; Calero, S. Understanding Water Adsorption in Cu-BTC Metal-Organic Frameworks. *J. Phys. Chem. C* **2008**, *112*, 15934–15939.
- (41) Martin, M. G.; Siepmann, J. I. Transferable Potentials for Phase Equilibria. 1. United-Atom Description of n-Alkanes. *J. Phys. Chem. B* **1998**, *102*, 2569–2577.
- (42) Wick, C. D.; Martin, M. G.; Siepmann, J. I. Transferable Potentials for Phase Equilibria. 4. United-atom Description of Linear and Branched Alkenes and Alkylbenzenes. *J. Phys. Chem. B* **2000**, *104*, 8008–8016.
- (43) Lamia, N.; Jorge, M.; Granato, M. A.; Paz, F. A. A.; Chevreau, H.; Rodrigues, A. E. Adsorption of Propane, Propylene and Isobutane on a Metal-Organic Framework: Molecular Simulation and Experiment. *Chem. Eng. Sci.* **2009**, *64*, 3246–3259.
- (44) Teo, H. W. B.; Chakraborty, A.; Kayal, S. Evaluation of CH_4 and CO_2 Adsorption on HKUST-1 and MIL-101(Cr) MOFs Employing Monte Carlo Simulation And Comparison With Experimental Data. *Appl. Therm. Eng.* **2017**, *110*, 891–900.
- (45) Gupta, A.; Chempath, S.; Sanborn, M. J.; Clark, L. A.; Snurr, R. Q. Object-oriented Programming Paradigms for Molecular Modeling. *Mol. Simul.* **2003**, *29*, 29–46.
- (46) Wolf, D.; Keblinski, P.; Phillpot, S. R.; Eggebrecht, J. Exact Method For The Simulation of Coulombic Systems By Spherically Truncated, Pairwise r^{-1} Summation. *J. Chem. Phys.* **1999**, *110*, 8254–8282.

- (47) Snurr, R. Q.; Bell, A. T.; Theodorou, D. N. Prediction of Adsorption of Aromatic Hydrocarbons in Silicalite from Grand Canonical Monte Carlo Simulations with Biased Insertions. *J. Phys. Chem.* **1993**, *97*, 13742–13752.
- (48) Peng, D. Y.; Robinson, D. B. A New Two-Constant Equation of State. *Ind. Eng. Chem. Fundam.* **1976**, *15*, 59–64.
- (49) Myers, A. L.; Monson, P. A. Adsorption in Porous Materials at High Pressure: Theory and Experiment. *Langmuir* **2002**, *18*, 10261–10273.
- (50) Ramalho, J. P. P.; Gomes, J. R. B.; Illas, F. Accounting for van der Waals Interactions Between Adsorbates and Surfaces in Density Functional Theory Based Calculations: Selected Examples. *RSC Adv.* **2013**, *3*, 13085–13100.
- (51) Walker, M.; Harvey, A. J. A.; Sen, A.; Dessent, C. E. H. Performance of M06, M06-2X, and M06-HF Density Functionals for Conformationally Flexible Anionic Clusters: M06 Functionals Perform Better than B3LYP for a Model System with Dispersion and Ionic Hydrogen-Bonding Interactions. *J. Phys. Chem. A* **2013**, *117*, 12590–12600.
- (52) Grimme, S. Semiempirical GGA-type Density Functional Constructed With A Long-Range Dispersion Correction. *J. Comput. Chem.* **2006**, *27*, 1787–1799.
- (53) Hutter, J.; Iannuzzi, M.; Schiffrmann, F.; VandeVondele, J. cp2k: Atomistic Simulations of Condensed Matter Systems. *Wiley Interdiscip. Rev. Comput. Mol. Sci.* **2014**, *4*, 15–25.
- (54) Krack, M. Pseudopotentials for H to Kr Optimized for Gradient-Corrected Exchange-Correlation Functionals. *Theor. Chem. Acc.* **2005**, *114*, 145–152.
- (55) Goedecker, S.; Teter, M.; Hutter, J. Separable Dual-space Gaussian Pseudopotentials. *Phys. Rev. B: Condens. Matter Mater. Phys.* **1996**, *54*, 1703–1710.
- (56) Hartwigsen, C.; Goedecker, S.; Hutter, J. Relativistic Separable Dual-space Gaussian Pseudopotentials from H to Rn. *Phys. Rev. B: Condens. Matter Mater. Phys.* **1998**, *58*, 3641–3662.
- (57) Boys, S.; Bernardi, F. The Calculation of Small Molecular Interactions By The Differences of Separate Total Energies. Some Procedures With Reduced Errors. *Mol. Phys.* **1970**, *19*, 553–566.
- (58) Giannozzi, P.; et al. Quantum Espresso: A Modular and Open-source Software Project for Quantum Simulations of Materials. *J. Phys.: Condens. Matter* **2009**, *21*, 395502.
- (59) Troullier, N.; Martins, J. L. Efficient pseudopotentials for plane-wave calculations. *Phys. Rev. B: Condens. Matter Mater. Phys.* **1991**, *43*, 1993–2006.
- (60) Weeks, J. D.; Chandler, D.; Andersen, H. C. Role of Repulsive Forces in Determining the Equilibrium Structure of Simple Liquids. *J. Chem. Phys.* **1971**, *54*, 5237–5247.
- (61) Chandler, D.; Weeks, J. D.; Andersen, H. C. Van der Waals Picture of Liquids, Solids, and Phase Transformations. *Science* **1983**, *220*, 787–794.